Antitumorigenesis of antioxidants in a transgenic Rac1 model of Kaposi's sarcoma

Qi Ma[a,b], Lucas E. Cavallin[c], Bin Yan[d], Shoukang Zhu[b], Elda Margarita Duran[c], Huili Wang[e], Laura P. Hale[f], Chunming Dong[b], Ethel Cesarman[g], Enrique A. Mesri[c,1], and Pascal J. Goldschmidt-Clermont[a,b,1]

[a]Vascular Biology Institute, [b]Department of Medicine, and [c]Viral Oncology Program, Sylvester Comprehensive Cancer Center and Department of Microbiology and Immunology, University of Miami Miller School of Medicine, Miami, FL 33136; [d]Department of Radiation Oncology, Virginia Commonwealth University Medical Center, Richmond, VA 23298; [e]Department of Pathology and Laboratory Medicine, University of North Carolina, Chapel Hill, NC 27599; [f]Department of Pathology, Duke University Medical Center, Durham, NC 27710; and [g]Department of Pathology and Laboratory Medicine, Weill Medical College of Cornell University, New York, NY 10065

Edited by Gregg L. Semenza, Johns Hopkins University School of Medicine, Baltimore, MD, and approved April 1, 2009 (received for review December 12, 2008)

Kaposi's sarcoma (KS) is the major AIDS-associated malignancy. It is characterized by the proliferation of spindle cells, inflammatory infiltrate, and aberrant angiogenesis caused by Kaposi's sarcoma herpesvirus (KSHV) infection. Small GTPase Rac1, an inflammatory signaling mediator triggering reactive oxygen species (ROS) production by NADPH-oxidases, is implicated in carcinogenesis and tumor angiogenesis. Here, we show that expression of a constitutively active Rac1 (RacCA) driven by the α-smooth muscle actin promoter in transgenic mice is sufficient to cause KS-like tumors through mechanisms involving ROS-driven proliferation, up-regulation of AKT signaling, and hypoxia-inducible factor 1-α–related angiogenesis. RacCA-induced tumors expressed KS phenotypic markers; displayed remarkable transcriptome overlap with KS lesions; and were, like KS, associated with male gender. The ROS scavenging agent *N*-acetyl-cysteine inhibited angiogenesis and completely abrogated transgenic RacCA tumor formation, indicating a causal role of ROS in tumorigenesis. Consistent with a pathogenic role in KS, immunohistochemical analysis revealed that Rac1 is overexpressed in KSHV$^+$ spindle cells of AIDS-KS biopsies. Our results demonstrate the direct oncogenicity of Rac1 and ROS and their contribution to a KS-like malignant phenotype, further underscoring the carcinogenic potential of oxidative stress in the context of chronic infection and inflammation. They define the RacCA transgenic mouse as a model suitable for studying the role of oxidative stress in the pathogenesis and therapy of KS, with relevance to other inflammation-related malignancies. Our findings suggest host and viral genes triggering Rac1 or ROS production as key determinants of KS onset and potential KS chemopreventive or therapeutic targets.

angiogenesis | chemoprevention | hypoxia-inducible factor 1-α | reactive oxygen species (ROS) | tumorigenesis

Kaposi's sarcoma (KS) is an angioproliferative malignancy of the skin and mucosa, which can also invade viscera in more disseminated cases, often leading to death (1–3). KS lesions display neovascularization, proliferation of spindle cells, and erythrocyte extravasation (1). Classic KS affects elderly men of Mediterranean or Eastern European Jewish ancestry. African endemic KS is frequently observed in equatorial Africa. Iatrogenic KS is associated with immunosuppression and is frequently found in transplant patients. Finally, epidemic KS is a major AIDS-defining malignancy that predominantly affects HIV-infected male homosexuals (1). Although KS incidence has decreased with the use of highly active antiretroviral therapy (HAART), KS still leads to significant mortality and morbidity in many HIV-infected patients (4). Compelling epidemiological, pathological, and molecular evidence indicates that infection with the γ-2 herpesvirus, Kaposi's sarcoma-associated herpesvirus (KSHV)/human herpesvirus-8, is required for KS carcinogenesis (2, 3). KSHV infection can lead to KS-like phenotypes in vitro and angiogenic tumor formation in vivo. Moreover, KSHV carries several genes that are able to induce spindle cell transformation and angiogenesis characteristic of KS, such as the viral G protein-coupled receptor (vGPCR) (5–7), viral IL-6, K1, K12, and viral macrophage inflammatory protein (2, 3, 8). The small GTPase Rac1, a member of the Rho family within the Ras superfamily, regulates a variety of cellular functions, including membrane ruffling (9), cell motility (10), actin polymerization (9), cadherin-mediated cell-cell adhesion (11), and ROS production, via members of the phagocytic as well as nonphagocytic NADPH-oxidase (NOX) family (12). Several studies have implicated a pathogenic role of Rac1 in tumor development (13, 14) and in angiogenic lesion formation by KSHV vGPCR (15). Rac-induced ROS have also been proven to mediate Ras-induced cell transformation (16). Rac1b, a constitutively active Rac1 splice variant expressed in some human cancers, has been shown to promote cellular transformation and to mediate matrix metalloproteinase-3–induced epithelial-mesenchymal transition and genomic instability (13, 14). Seeking to investigate the biological effects of Rac1 activation in vivo in cells of the vascular wall, we established FVB/N transgenic mouse lines that express constitutively active Rac1 (V12 mutant or RacCA) under the control of the α-smooth muscle actin (α-SMA) promoter. These mice showed hypertension (17) and accelerated wound healing (18). Here, we show that as transgenic mice aged, they developed KS lesions in a ROS-dependent manner.

Results

Transgenic Mice Expressing Constitutively Active Rac1 Develop Tumors Resembling KS. We found that a significant portion of transgenic RacCA mice would develop discolored reddish lesions, mainly on the tail, starting at 8 months of age (Fig. 1 *A* and *B*). Tumorigenesis increased with age, transgene dose, and male gender [Fig. 1*F* and supporting information (SI) Fig. S1]. Female transgenic mice developed tumors later in life (mean age = 18 months). No tumor formation was observed in WT littermates ($n = 79$). Histological examination of the tumors revealed many similarities to human KS; both were characterized by excessive proliferation of spindle cells without identifiable organized vascular structures inside the tumors, but with slits containing red blood cells and hemosiderin between the cells (Fig. 1 *D* and *E*). RacCA spindle cells also stained positive for CD31, CD34, von Willebrand factor (vWF), and α-SMA, which are the characteristic phenotypic markers of KS lesions (Fig. S2). Transgene expression in the tumors was demonstrated by a Rac1 transgene-specific RT-PCR assay (data

Author contributions: E.C., E.A.M., and P.J.G.-C. designed research; Q.M., L.E.C., B.Y., S.Z., E.M.D., and H.W. performed research; E.C. contributed new reagents/analytical tools; Q.M., L.E.C., B.Y., E.M.D., L.P.H., C.D., E.A.M., and P.J.G.-C. analyzed data; and Q.M., E.A.M., and P.J.G.-C. wrote the paper.

The authors declare no conflict of interest.

This article is a PNAS Direct Submission.

Freely available online through the PNAS open access option.

[1]To whom correspondence may be addressed. E-mail: emesri@med.miami.edu or pgoldschmidt@med.miami.edu.

This article contains supporting information online at www.pnas.org/cgi/content/full/0812688106/DCSupplemental.

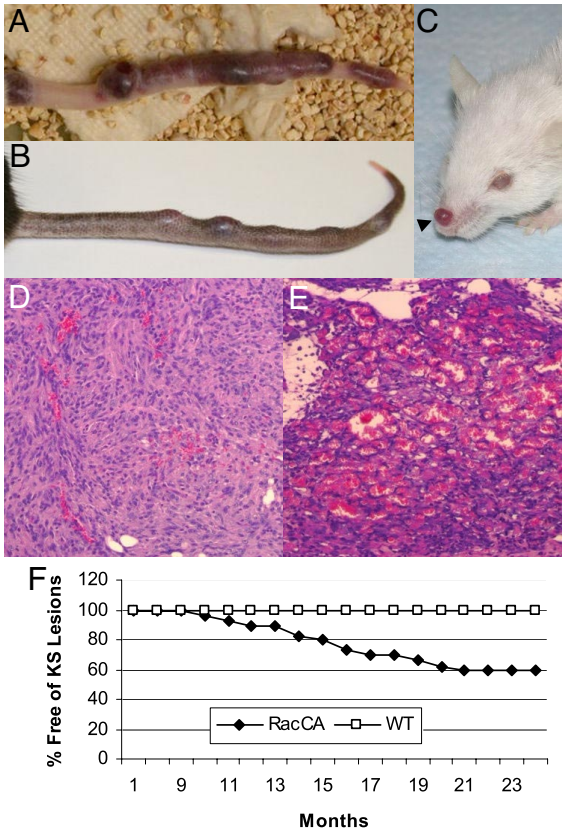

Fig. 1. KS-like tumorigenesis in RacCA transgenic mice. (*A*) Macroscopic image of a representative tail tumor in a male RacCA$^{+/+}$ mouse from the FVB/N strain. (*B*) Tail KS-like tumor in a male RacCA$^{+/+}$ mouse from the C57BL/6 strain. (*C*) KS-like tumor on the nose of a RacCA$^{+/+}$ mouse (FVB/N). H&E staining of tumor tissues from an early-stage RacCA tumor (*D*) and a late-stage RacCA tumor (*E*). (*F*) Tumor-free survival of homozygous male RacCA mice.

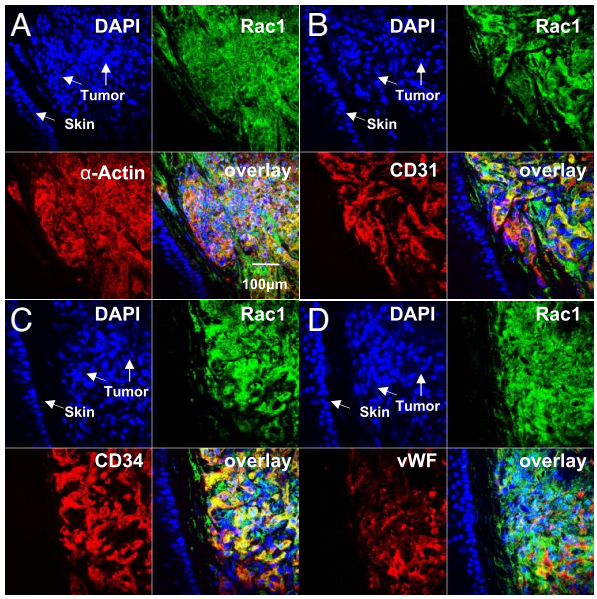

Fig. 2. Immunophenotype of the RacCA tumor tissue. Immunofluorescence double staining showing colocalization of Rac1– and α-SMC-actin–expressing cells with KS markers CD31, CD34, and vWF.

not shown) and immunofluorescence double staining for Rac1. Tumor cells coexpressed Rac1 and α-SMA as expected for a RacCA transgene driven by the α-SMA promoter (Fig. 2). Moreover, Rac1-positive tumor cells were also positive for the KS phenotypic markers CD31 and CD34. These data are consistent with KS-like tumors being a consequence of Rac1 transgenic expression.

Transcriptional Profiling of RacCA Tumors. Molecular signatures are a useful way to evaluate the phenotypic identity of tumors. The KS molecular signature was recently established by identifying 1,256 KS genes that differentiate KS versus normal skin sample groups (19). Similarly, we have recently established the KS-like signature of mouse tumors induced by cells transfected with a bacterial artificial chromosome encoding the whole KSHV infectious genome [mECK36 tumors = KSHV-induced mouse KS-like (KSHV-mKS) tumors] (7). To evaluate the extent to which the RacCA-induced mouse KS-like (RacCA-mKS) tumors mimic KS and KSHV-mKS signatures, we determined the transcriptional profile of RacCA tumors using gene expression arrays and we sought genes from the KS and KSHV-mKS signatures that were able to differentiate RacCA tumors from normal mouse skin ($P < 0.05$). Orthologs of 723 genes from the human KS signature were surveyed in the Affymetrix mouse 430 2.0 chip. Four hundred fifty of the 723 KS signature genes were found to be significantly up- or down-regulated when comparing RacCA tumor versus normal skin ($P < 0.05$). Of those 450 genes, a total of 408 genes were similarly up- or down-regulated in RacCA tumors and KS, and 398 of these genes displayed similar up- or down-regulation as for KSHV-mKS tumors (Fig. 3 *A* and *B*). Such results indicate that the RacCA tumor shares

Fig. 3. Global gene expression of RacCA tumors resembles KS and KSHV-induced Kaposi-like mouse tumors. (*A*) Heat map representation of 450 significantly up- or down-regulated genes ($P < 0.05$) from the 723 human KS signature genes that were present on the Affymetrix mouse 430 2.0 chip. A total of 408 genes (91%) in this 408-gene signature were equally up- or down-regulated between RacCA-mKS and KS sample groups. Control mouse and human SCC samples possess less than 10% of the KS signatures. Selected up- (red) or down-regulated (blue) genes are listed on the right. The full list of genes is available in Table S2. (*B*) Distribution of KS signature. Dark gray, genes shared by KS, RacCA-mKS, and KSHV-mKS; orange, genes shared by KS and RacCA-mKS; green, genes shared by KS and KSHV-mKS; yellow, genes in KS only. Gene list is available in Table S3. (*C*) Up-regulation of angiogenic gene expression in RacCA tumors compared with surrounding uninvolved tissue. Bars represent mean fold increase (triplicates ± SEM) in mRNA levels quantified by real-time quantitative RT-PCR.

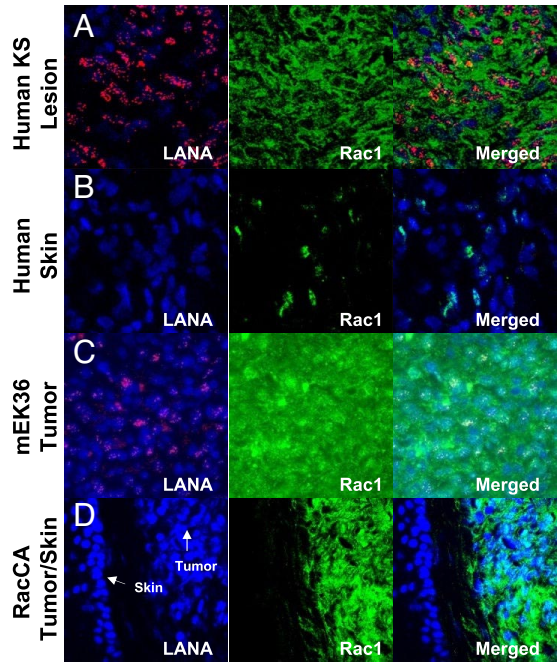

Fig. 4. Rac1 is overexpressed in AIDS-KS, mECK36 (KSHV-mKS), and RacCA-mKS tumors. Immunofluorescence detection of Rac1 and KSHV LANA expression in AIDS-KS tumor biopsies (*A*), KSHV-mKS (mECK36 tumors) (*C*), and RacCA tumors (*D*) compared with normal human skin tissue (*B*) and mouse skin tissue (*D*).

56% of the KS molecular signature and 58% of the KSHV-mKS signature (691 genes), respectively. As a comparison, the human skin squamous cell carcinoma (SCC) signature and a mouse SCC model signature, which are also defined by comparison with skin, shared only 8.4% and 6.4% of the KS signatures, respectively (20, 21) (Fig. 3*A*). The 56% signature overlap between RacCA-mKS with KSHV-mKS and KS suggests a major contribution of Rac activation to the KS phenotype and further defines RacCA-mKS as an intriguing murine model for KS derived from a single host oncogene expression.

AIDS-Associated KS Tumors Overexpress Rac1. Molecular signatures are composed of genes critical for the malignant phenotype. Thus, the more than 50% overlap between the transcriptional signatures of tumors induced by RacCA with those induced by KSHV and with human KS suggests that activation of Rac1 could play a key role in KS. As genes involved in tumorigenesis tend to be selected for overexpression in tumors, we determined the levels of Rac1 staining and the latency-associated nuclear antigen (LANA) of KSHV in 4 human AIDS-KS tumor biopsies and in mECK36 tumors (Fig. 4 *A* and *C*). We found a high level of Rac1 expression in all $LANA^+$ cells of the lesions and tumors compared with the adjacent skin that just displayed limited patchy foci of Rac1 expression (Fig. 4 *B* and *D*).

Molecular Mechanisms of Angiogenesis Activation and Cell Proliferation in RacCA-mKS Tumors. Because angiogenic activation is a major hallmark of KS pathogenesis, we determined by quantitative RT-PCR the levels of angiogenic growth factors and receptors in the tumors relative to normal skin. We found that RacCA tumors up-regulate VEGF receptors 1 and 2 and show up-regulation of the angiogenesis factor most up-regulated in human KS (22), angiopoietin 2, and its receptor Tek (Fig. 3*C*). This pattern of expression is indicative of paracrine and autocrine angiogenic activities in RacCA tumors. To explore the mechanism underpinning spindle cell proliferation, we studied cells explanted from RacCA tumors using vascular smooth muscle cells (SMCs) from the same mice as a control. Explanted cells lacked contact inhibition (data not shown). Because cytokines play an important role in KS progression and are expressed in cultured KS cells (23), we characterized cytokine secretion. Explanted RacCA-mKS spindle cells secreted high levels of chemocytokines and angiogenic factors, typical of explanted human KS spindle cells, including IL-6, IL-8, TNF-α, monocyte chemoattractant protein-1 (MCP-1), macrophage inflammatory protein-1-alpha (MIP1α), and keratinocyte-derived chemokine (KC) (Table S1). Reduction of cytokine levels in the media by media replacement without addition of conditioned media factors led to cell death (data not shown), suggestive of autocrine activities in RacCA tumor cells.

Genetic Instability in RacCA Tumors. A hallmark of most human cancers, genomic instability has also been frequently reported in KS (24, 25). Rac1 has been shown to induce genomic instability through ROS (13). Additionally, as a modulator of cytoskeleton organization, Rac1 activation could cause a defect in cytokinesis during mitosis, leading to polyploidy and aneuploidy. We found increased levels of DNA oxidative damage, as evidenced by the 8-oxo-dG staining and increased phospho-H2AX (γ-H2AX) foci in the nuclei of tumor cells (Fig. S3 *A–F*), which is suggestive of ROS-mediated oxidative DNA damage in RacCA tumors. In RacCA tumor primary cultures, aberrant chromosomes were frequently observed, at a frequency varying between 5 and 10% (Fig. S3 *G–I*). Less than 2% of chromosome aberrance was observed in the control WT SMCs. ModiFit FACS (Becton Dickinson) analysis showed significant presence of polyploidy and aneuploidy in RacCA tumor primary culture (data not shown), which is also demonstrated by manually counting chromosome spreads (Fig. S3*K*). *p*53 expression and function are essential for avoiding proliferation of cells with damaged genomes. Interestingly, 67% of RacCA tumor cases examined so far showed complete loss of *p*53 expression, suggesting a possible mechanism underlying RacCA-induced genetic instability (Fig. S3*J*). KS tumors could have both cell-autonomous and paracrine or reactive components (1). Although mammal cells need more than a single oncogenic hit to become fully transformed, the occurrence of RacCA tumors along with evidence of genetic instability suggests that the oxidative DNA damage process initiated by RacCA could lead to full cell transformation. To assess the presence of transformed cells within RacCA tumors, we carried out an anchorage-independent growth assay. RacCA tumor-explanted cells formed colonies in soft agar, whereas normal SMCs did not (Fig. 5*G*). Taken together, our data indicate that the RacCA transgene recapitulates a KS-like tumorigenic process involving oxidative DNA damage, leading to genetic instability and full cellular transformation.

RacCA Tumors Display Enhanced AKT Expression and Activation. Full transformation and tumorigenesis involve a combination of pro-survival and proliferative activities. Rac1 is known to activate AKT through the PI3K pathway in many cell types (26). Using gene expression data, we showed that in the tumor tissue, the expression of AKT1 and AKT3 are consistently 2.2- and 5.4-fold higher, respectively, relative to intact tail tissue from WT control mice (Fig. 5*A*). AKT activity measured by a Meso Scale Discovery (MSD) multispot assay demonstrated increased overall AKT phosphorylation in tumor tissue compared with the SMC controls and skin (Fig. 5*B*). ROS are thought to affect proteins with low pK_a cysteine residues, such as protein tyrosine phosphatase (PTEN), which functions as a tumor suppressor by negatively modulating the PI3K-AKT signaling pathway. We examined the possibility of inactivation of PTEN as a result of increased oxidative stress in our RacCA mice. Immunoprecipitated PTEN activity from various mouse tissues was compared using a malachite green assay. We exposed PTEN to exogenous H_2O_2 and found that its activity decreased in a concentration-dependent manner indicative of oxidative sensitivity (data not shown). We then found that PTEN activity is reduced in all RacCA tumor tissue compared with normal mouse tissue (Fig. 5*C*), with the highest reduction in activity found in tumor tissues. Our results suggest that PTEN inactivation by ROS

might be coupled with increased AKT activity in RacCA tumors and may play a role in the KS tumorigenic mechanism. These results suggest that ROS-mediated AKT activation in RacCA may contribute to prosurvival activities leading to KS-like tumorigenesis.

Causal Role of ROS in RacCA Tumorigenesis. We further sought to prove the role of ROS in proliferation of RacCA spindle cells. Previously, we had shown the contribution of Rac1 and ROS to the unchecked mitogenic activity of v-H-Ras–transformed fibroblasts (27). RacCA mice produce excessive amounts of $\cdot O_2^-$ in their SMCs (17). Excessive $\cdot O_2^-$ production is known to cause oxidative DNA damage and genome instability (13, 28), to transform cells in culture (29), and to potentiate tumor progression (30). To determine if increased $\cdot O_2^-$ production could be a contributor to RacCA tumorigenicity, we measured $\cdot O_2^-$ levels in the tumor (Fig. 5*D*). A 2-fold increase in $\cdot O_2^-$ production was observed in tumor tissue compared with normal skin tissue obtained from WT mouse tail. In accordance with a critical role for Rac1 in ROS production, no change in mRNA levels was observed in all major subunits of NOX, including NOX1, NOX2, NOX4, $p22^{PHOX}$, $p47^{PHOX}$, $p67^{PHOX}$, NOXO1, and NOXA1, indicating that the increase in ROS production was likely attributable to Rac1 constitutive activity and unlikely attributable to differences in NOX levels. To establish the role of ROS in mediating proliferation of RacCA tumor cells further, we cultured tumor cells in the absence and presence of *N*-acetyl-cysteine (NAC) or H_2O_2. Addition of 10 mM NAC to the media substantially inhibited cell proliferation, whereas H_2O_2 further stimulated cell growth relative to untreated tumor cells (Fig. 5*E*). These data suggest that ROS contribute to RacCA-induced cell proliferation. To determine whether or not the increased AKT activation in RacCA was linked to ROS, we determined ratios of AKT phosphorylation in the presence and absence of NAC. As shown in Fig. 5*F*, NAC treatment led to a dose-dependent reduction in AKT phosphorylation in explanted RacCA tumor cells. KS tumorigenicity is characterized by angiogenic activation. Rac1, AKT, and ROS are thought to modulate VEGF angiogenesis via hypoxia-inducible factor 1 (HIF1) (31). Fig. 5*J* shows that there is an increase of HIF1-α protein level in RacCA tumors that correlated with increased levels of VEGF secretion by RacCA tumor cells in vitro. As shown in Fig. 5 *H* and *K*, NAC treatment reduced HIF-1α levels and concomitantly reduced VEGF secretion to basal levels. The link between ROS, proliferation, AKT, and angiogenicity indicates that these oxidative stress mediators should be critical for RacCA tumorigenesis. Two important pieces of evidence indicate that this is the case. NAC completely suppressed anchorage-independent growth of RacCA tumor cells, and NAC delivered in drinking water throughout the growth of transgenic animals completely prevented the development of KS-like tumors. As shown in Fig. 5*I*, RacCA transgenic mice controls (no NAC in drinking water) developed KS-like tumors to an incidence consistent with that observed in other experiments. On the other hand, animals that received NAC in the drinking water did not develop any detectable tumors. To determine the role of ROS in maintenance of the RacCA-induced malignant phenotype, we randomized 6 tumor-bearing mice that did not receive NAC to a 3-month placebo or NAC treatment. We found that in contrast to placebo-receiving mice in which tail tumors almost duplicated in size, NAC-treated animals did not show signs of further tumor growth, suggesting that ROS are implicated in RacCA tumor cell proliferation (Fig. 5*L*). These results show a causal connection between ROS and Rac1-induced KS-like tumorigenesis. Moreover, they serve as proof of principle for the use of nontoxic antioxidants such as NAC as potential chemopreventive agents that can be used to block the contribution of oxidative stress to KS tumorigenesis.

Discussion

The ability of activated Rac1 to generate KS-like tumors and its overexpression in AIDS-KS lesions suggest that Rac1 activation

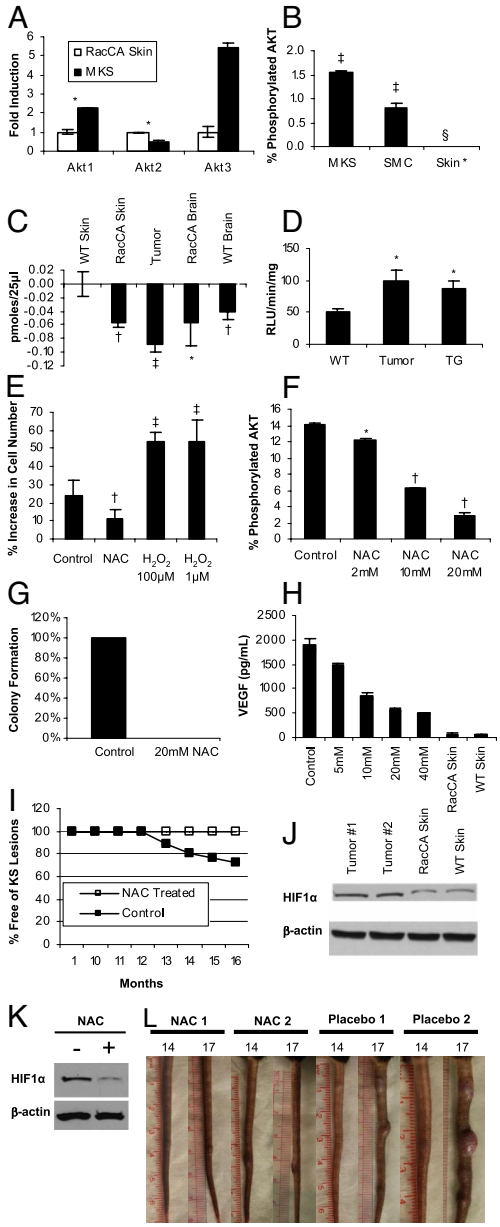

Fig. 5. Causal role of ROS in RacCA tumorigenesis. (*A*) Up-regulation of AKT isoform gene expression in RacCA tumors compared with uninvolved adjacent tissues. Bars represent mean fold increase (triplicates ± SEM) in mRNA levels quantified by real-time quantitative RT-PCR. (*B*) AKT phosphorylation levels (as percentage of AKT phosphorylated/total AKT signal) in RacCA tumor compared with smooth muscle and skin tissue, as determined by MSD (duplicate ± SEM; see *Materials and Methods*). (*C*) Activities of immunoprecipitated PTEN from various tissues measured by release of free phosphate (see *Materials and Methods*) (triplicates ± SEM). (*D*) Lucigenin luminescence determination of ($\cdot O_2^-$) production in the tumor tissue and adjacent skin tissue compared with the tail skin tissue from WT mice skin tissue (triplicates ± SEM). (*E*) Effects on cell proliferation of NAC (10 mM) or H_2O_2 (1 μM and 100 μM). Bars show percentage increase in cell number after 24 h of incubation (triplicates ± SEM). (*F*) Dose-dependent inhibition of AKT phosphorylation in cultured RacCA tumor cells by NAC (as percentage of AKT phosphorylated/total AKT signal) determined by MSD (duplicate ± SEM). (*G*) Effect of NAC (20 mM) on colony-forming ability of cultured RacCA tumor cells. (*H*) Dose-dependent reduction of VEGF secretion by 24 h of NAC treatment in cultured RacCA tumor cells. (*I*) Oral administration of NAC (10 mg/mL in drinking water) prevents tumor formation in homozygous RacCA mice. (*J*) Western blot showing increased HIF1-α level in RacCA tumor tissue (T1, T2). (*K*) NAC treatment (10 mM) reduced HIF1-α level in cultured RacCA tumor cells after 24 h. (*L*) Three months of oral administration of NAC after tumor onset (14 months) stabilized tumor progression. Significance was established by *t* test: $^*P < 0.05$; $^\dagger P < 0.01$; $^\ddagger P < 0.001$; §total AKT detection did not surpass background levels.

leading to ROS production is carcinogenic and could play a major role in KS pathogenesis. The direct tumorigenic role of ROS in Rac1-induced KS-like tumorigenesis and the possibility of preventing it with nontoxic antioxidants emphasize the importance of oxidative stress and its modulation for KS etiology, prevention, and therapy.

NAC inhibition of RacCA tumor formation indicates an etiological role for Rac-mediated ROS production. Although RacCA tumors were predominantly found on tails, similar histological changes were also observed on paws, ears, and noses in separate mice (Fig. 1*C*). These areas represent differentiated skin tissues, with sparse hair coverage, a feature that might subject the skin to excessive exposure to light (UV) and other injuries (excoriations), rendering the exposed cells more susceptible to oxidative damage, and therefore more likely to experience Rac1-mediated transformation. An oxidative damage etiology may also explain the gender bias of Rac1 tumorigenicity, because it was shown that oxidative damage to mitochondrial DNA in male mice was 4-fold higher than that in female mice because of better antioxidant capacity of female mitochondria (32).

Our results are consistent with prior studies with a constitutively activated Rac1 (Rac1QL) expression in endothelial cells (15). Yet, the convergence of phenotypes of transgenes driven by endothelial and vascular smooth muscle-specific promoters leads to interesting questions for the pathogenesis of KS, for which the cellular origin remains unclear (1). Our animal model points to the existence of a potential α-SMA–expressing KS spindle cell progenitor, which is consistent with the fact that most clinical KS samples are positive for α-SMA (33). In adult animals, α-SMA gene expression is highly restricted to smooth muscle, smooth muscle-like cells, and myofibroblasts that are typically present in tissues subjected to mechanical stress. Myofibroblasts become prominent under certain pathological situations such as wound healing (34). Unsupervised clustering of the RacCA tumor transcriptome with those of different mouse cell types placed it between SMCs and fibroblasts (Fig. S4), which is suggestive of a myofibroblast lineage (35). It is tempting to speculate that an α-SMA–expressing cell, particularly a common endothelial-SM vascular progenitor, could be a primary cell for the RacCA-induced KS-like tumor, and possibly also a KS progenitor cell (35).

Because it was shown that KSHV vGPCR mediates KS-like tumorigenicity via Rac1 (15), our results are consistent with reported vGPCR transgenic models of KS-like tumorigenesis (6, 7) and with the critical role that vGPCR appears to play in KSHV-induced carcinogenesis of KS (7, 8, 15). Our finding that Rac1 is overexpressed in KSHV-infected spindle cells places Rac1 at the center of KS pathogenesis. Genes that are critical for tumor biology tend to become selected during carcinogenesis. Thus, the overexpression of Rac1 in the AIDS-KS lesions, together with the 56% overlap in the transcriptome, points to a critical role for Rac1 activation in KS. The fact that all $LANA^+$ cells of the lesion overexpress Rac1 suggests that this gene is engaged in direct and paracrine KSHV-induced angiogenesis and spindle cell proliferation. This is consistent with Rac1 playing a key role not only in the minority of lytically infected cells that express vGPCR but in latently infected $vGPCR^-$ cells that are paracrinally stimulated by vGPCR-expressing cells that secrete angiogenic growth factors and chemokines known to mediate its biological activities via Rac1.

Our data support 3 levels of impact of Rac1 activation of ROS in our RacCA mouse model. First, through inhibition of PTEN, AKT-mediated survival of tumor cells is enhanced, consistent with our prior report (27). Second, ROS-induced chromatin oxidation and DNA damage lead to loss of gatekeeper tumor suppressor genes like *p*53. Finally, ROS-mediated up-regulation of HIF1-α leads to activation of VEGF expression and angiogenesis. The concurrence of these processes may be critical to tumor formation in RacCA-induced KS, with variable levels. Our results showing the carcinogenicity of constitutive Rac activation are not only relevant to KS but to the emerging array of malignancies in which a link with infection or inflammation has been proven through epidemiological and experimental evidence. They include virally induced cancers such as hepatocellular carcinoma induced by chronic hepatitis B virus infection, gastric carcinoma induced by chronic *Helicobacter pylori* infection, and a vast array of noninfectious human cancers in which inflammatory cells and cytokines have been shown to be integral to the carcinogenic process. Our results show that chronic activation of the Rac1 pathway can act as a source for carcinogenic ROS in many human cancers. The RacCA tumor model is unique in that it is driven solely by this pathway. Therefore, it could constitute an important tool for seeking therapeutic and chemopreventive interventions.

The inhibition of RacCA tumorigenesis by NAC demonstrates the causal link between oxidative stress and Rac1 tumorigenicity and is consistent with recent findings showing the ability of NAC to prevent myc-induced tumorigenesis by blocking ROS-induced HIF1-α stabilization (36). Our results reinforce previous studies showing NAC inhibition of KS spindle cell angiogenesis (37). Our results serve as proof of principle for the use nontoxic antioxidants, such as NAC, as potential chemopreventive agents that can be used to block the contribution of oxidative stress to tumorigenesis. Our results showing that NAC prevented further growth of RacCA established tumors (Fig. 5*L*) suggest that antioxidants could act as tumoristatic agents and would be a valuable nontoxic adjuvant to cytotoxic therapies. We propose that NAC preparations approved by the U.S. Food and Drug Administration (FDA) (38), or other prescription drugs that function by inhibiting ROS and their production by NOX enzymes, may be effective for chemoprevention and therapy of KS as well as other inflammation-related cancers. These unique concepts warrant testing in the context of robust preclinical and clinical studies.

Although the incidence of KS has declined since the introduction of HAART, it remains the most common malignancy among HIV-infected individuals in the Western world and in many developing countries, especially in Africa. Importantly, KS is still an incurable disease (4). RacCA mice define a valuable resource for KS research, providing a model for the development and testing of innovative therapeutic approaches, particularly therapeutic or chemopreventive strategies that involve the use of selective antioxidants. Our results implicating Rac1 in KS tumorigenesis and its expression in AIDS-KS lesions define Rac1 and its downstream pathways of oxidative stress as attractive innovative targets for both targeted and antioxidant therapies.

Materials and Methods

Generation of RacCA Transgenic Mice. The method was described previously (18). Transgenic mice were screened by PCR. Real-time PCR was performed to identify the homozygosity and heterozygosity of the transgenic mice using an ABI 7700 Sequence Detector (Applied Biosystems). Rodent GAPDH was used as an internal control.

Animal Treatment. Fifty age-matched, homozygous, RacCA C57BL/6 mice were randomized to 2 identical groups on weaning. The active treatment group ($n = 25$) received 10 g/L NAC in their drinking water, freshly prepared every other day and provided ad libitum. The control group ($n = 25$) received regular drinking water without NAC. Mice were observed for tumor development during their entire life span. In another experiment, 6 male tumor-bearing RacCA mice were randomized to 2 matched groups ($n = 3$ each), one receiving NAC (1 g/L) in their drinking water and the other receiving untreated water (control group). Tumor growth was measured weekly with a caliper. One mouse in each group died attributable to non–tumor-related causes during the study. It is not unusual for C57BL/6 mice to become frail and occasionally die at the age of 17 months or older, unrelated to applied treatment. All animal experiments were submitted to and approved by the University of Miami Institutional Animal Care and Use Committee.

Histology, Immunohistochemistry, and Immuofluorescence. For histological studies on mouse tissue, formalin-fixed paraffin-embedded slides were stained with H&E, dehydrated, and mounted with Permount (Biomeda). Immunohistochemistry and immunofluorescence were performed on either formalin-fixed paraffin-embedded sections or frozen sections depending on the applicability of the antibody. Frozen sections of human KS lesion biopsy specimens were obtained from the tissue repository of the Department of Pathology and Laboratory Medicine at the New York Presbyterian Hospital–Weill Cornell Medical Center.

Please refer to *SI Materials and Methods* for assay details for this and successive method descriptions.

Cell Culture. Tumor tissue was excised under a dissecting microscope and minced. Primary culture was maintained in DMEM (Aldrich) and 10% FBS (GIBCO) with a half-medium change every 3 days.

Cell Proliferation Assay. Cell proliferation in the presence and absence of NAC and H_2O_2 was analyzed using a Cell Proliferation Assay Kit (Chemicon) following the manufacturer's instructions. A total of 10^5 tumor cells were treated for 24 h with 10 mM NAC or H_2O_2 at 100 μM and 1 μM in the media. Tumor cells maintained in normal medium were used as the control.

Cytokine Measurement. Culture medium (100 μL) was collected from 2-day cultures of RacCA tumor cells and mouse SMCs. Measurement was performed using a LINCOplex kit (LINCO Research, Inc.) following the manufacturer's protocol.

PTEN Malachite Green Assay. PTEN was immunoprecipitated from various mouse tissues using anti-PTEN antibody (Upstate) and protein A/G agarose beads (PIERCE). Four hundred micrograms of tissue lysate/sample was used. The PTEN malachite green assay (Upstate) was performed with bead-bound PTEN following the manufacturer's instructions. PTEN activity was measured in the amount (picomoles) of phosphate released per 25 μL reaction volume.

Phospho-AKT Assay. Levels of phospho (Ser 473)/total AKT were measured using a Whole Cell Lysate Kit (MultiSpot Assay System) from Meso Scale Discovery. The assay was performed according to the manufacturer's instructions, with duplicates of 20 μg of total protein from mouse tissue or cell culture.

Lucigenin Assay. The lucigenin assay was performed as previously described (39). Briefly, mouse thoracic aortas were dissected into 5-mm segments with extra adventitial tissue removed. Aortas were equilibrated in Krebs-Hepes buffer (millimolar content: NaCl, 99.01; KCl, 4.69; $CaCl_2$, 1.87; $MgSO_4$, 1.20; K_2HPO_4, 1.03; $NaHCO_3$, 25.0; Na-Hepes, 20.0; and glucose, 11.1) gassed with 95% O_2/5% CO_2 for 30 min at 37 °C. Vials with 1 mL of buffer with 100 μM lucigenin were placed in a Lumat LB9507 luminometer (Berthold Technologies). After 15 min of dark adaptation, background readings were recorded. Aorta segments were added to the vial. Luminescence readings were recorded at 5-sec intervals over 20 min. Respective background readings were subtracted. Aorta segments were rinsed with distilled H_2O and placed in a 90 °C oven overnight, and dry weight was measured. $\cdot O_2^-$ production was expressed as relative light units per minute per milligram of tissue dry weight.

Microarray. Total RNA was purified from tumor tissue, surrounding normal skin tissue, and WT tail skin tissue using a QIAGEN RNeasy kit (Qiagen). A Mouse Genome 430 2.0 Array (Affymetrix) was used to evaluate the expression level of over 39,000 transcripts with 45,037 probe sets. The integrity of RNA was confirmed with a Bioanalyzer 2100 (Agilent Technologies). cRNA was synthesized, labeled, and hybridized onto arrays at Duke University Microarray Facility according to standard Affymetrix methods. Raw data intensity profiles were analyzed using GeneSpring 7 (Agilent Technologies) to perform microarray normalization and statistical analysis. Statistically significant genes were selected by an ANOVA test to obtain the largest gene list that gave a false discovery rate of $<1\%$ (40). Significantly expressed genes were clustered with GeneSpring 7 using the Pearson correlation method.

Statistical Analysis. A Student's test was applied for the statistical determinations. $P < 0.05$ was considered significant. All experiments were repeated at least 3 times.

SI Materials and Methods. Please refer to *SI Materials and Methods* for further details and description of histology, immunohistochemistry, immunofluorescence, chromosomal aberration analysis, soft agar assay, flow cytometric analysis, RT-PCR), nested PCR, primer sequences, and PCR conditions.

ACKNOWLEDGMENTS. We thank Dr. Hamdy Hassanian for his invaluable contribution to the generation and characterization of the FBV/N transgenic mice expressing RacCA (17, 18). We thank Dr. Xialin Liu for her technical assistance and Carl Stone for his help on animal maintenance. This work was supported by a Grant HL71536–08 (to P.J.G.) and Grant CA75918 (to E.A.M.) from the National Institutes of Health. We would like to dedicate this study to our dear friend and esteemed colleague, Dr. William Harrington, Jr. (1954–2009), founder and Co-Director of the University of Miami Sylvester Cancer Center's Viral Oncology Program, which recruited and funded the E. A. Mesri laboratory and made this project possible.

1. Gallo RC (1998) The enigmas of Kaposi's sarcoma. *Science* 282:1837–1839.
2. Boshoff C, Weiss RA (1998) Kaposi's sarcoma-associated herpesvirus. *Adv Cancer Res* 75:57–86.
3. Ganem D (1997) KSHV and Kaposi's sarcoma: The end of the beginning? *Cell* 91:157–160.
4. Mitsuyasu RT (2000) AIDS-related Kaposi's sarcoma: Current treatment options, future trends. *Oncology (Huntingt)* 14:867–878; discussion 878, 881–883, 887.
5. Bais C, Santomasso B, Coso O, et al. (1998) G-protein-coupled receptor of Kaposi's sarcoma-associated herpesvirus is a viral oncogene and angiogenesis activator. *Nature* 391:86–89.
6. Yang TY, Chen SC, Leach MW, et al. (2000) Transgenic expression of the chemokine receptor encoded by human herpesvirus 8 induces an angioproliferative disease resembling Kaposi's sarcoma. *J Exp Med* 191:445–454.
7. Mutlu AD, Cavallin LE, Vincent L, et al. (2007) In vivo-restricted and reversible malignancy induced by human herpesvirus-8 KSHV: A cell and animal model of virally induced Kaposi's sarcoma. *Cancer Cells* 11:245–258.
8. Montaner S, Sodhi A, Molinolo A, et al. (2003) Endothelial infection with KSHV genes in vivo reveals that vGPCR initiates Kaposi's sarcomagenesis and can promote the tumorigenic potential of viral latent genes. *Cancer Cells* 3:23–36.
9. Hall A (1998) Rho GTPases and the actin cytoskeleton. *Science* 279:509–514.
10. Ridley AJ, Comoglio PM, Hall A (1995) Regulation of scatter factor/hepatocyte growth factor responses by Ras, Rac, and Rho in MDCK cells. *Mol Cell Biol* 15:1110–1122.
11. Braga VM, Machesky LM, Hall A, Hotchin NA (1997) The small GTPases Rho and Rac are required for the establishment of cadherin-dependent cell-cell contacts. *J Cell Biol* 137:1421–1431.
12. Abo A, Pick E, Hall A, et al. (1991) Activation of the NADPH oxidase involves the small GTP-binding protein p21rac1. *Nature* 353:668–670.
13. Radisky DC, Levy DD, Littlepage LE, et al. (2005) Rac1b and reactive oxygen species mediate MMP-3-induced EMT and genomic instability. *Nature* 436:123–127.
14. Singh A, Karnoub AE, Palmby TR, et al. (2004) Rac1b, a tumor associated, constitutively active Rac1 splice variant, promotes cellular transformation. *Oncogene* 23:9369–9380.
15. Montaner S, Sodhi A, Servitja JM, et al. (2004) The small GTPase Rac1 links the Kaposi sarcoma-associated herpesvirus vGPCR to cytokine secretion and paracrine neoplasia. *Blood* 104:2903–2911.
16. Qiu RG, Chen J, Kirn D, McCormick F, Symons M (1995) An essential role for Rac in Ras transformation. *Nature* 374:457–459.
17. Hassanain HH, Gregg D, Marcelo ML, et al. (2007) Hypertension caused by transgenic overexpression of rac1. *Antioxid Redox Signal* 9:91–100.
18. Hassanain HH, Irshaid F, Wisel S, et al. (2005) Smooth muscle cell expression of a constitutive active form of human Rac 1 accelerates cutaneous wound repair. *Surgery* 137:92–101.
19. Wang HW, Trotter MW, Lagos D, et al. (2004) Kaposi sarcoma herpesvirus-induced cellular reprogramming contributes to the lymphatic endothelial gene expression in Kaposi sarcoma. *Nat Genet* 36:687–693.
20. Martinez-Cruz AB, Santos M, Lara MF, et al. (2008) Spontaneous squamous cell carcinoma induced by the somatic inactivation of retinoblastoma and Trp53 tumor suppressors. *Cancer Res* 68:683–692.
21. Nindl I, Dang C, Forschner T, et al. (2006) Identification of differentially expressed genes in cutaneous squamous cell carcinoma by microarray expression profiling. *Mol Cancer* 5:30.
22. Brown LF, Dezube BJ, Tognazzi K, Dvorak HF, Yancopoulos GD (2000) Expression of Tie1, Tie2, and angiopoietins 1, 2, and 4 in Kaposi's sarcoma and cutaneous angiosarcoma. *Am J Pathol* 156:2179–2183.
23. Miles SA, Rezai AR, Salazar-Gonzalez JF, et al. (1990) AIDS Kaposi sarcoma-derived cells produce and respond to interleukin 6. *Proc Natl Acad Sci USA* 87:4068–4072.
24. Pyakurel P, Montag U, Castanos-Velez E, et al. (2006) CGH of microdissected Kaposi's sarcoma lesions reveals recurrent loss of chromosome Y in early and additional chromosomal changes in late tumour stages. *AIDS* 20:1805–1812.
25. Pan H, Zhou F, Gao SJ (2004) Kaposi's sarcoma-associated herpesvirus induction of chromosome instability in primary human endothelial cells. *Cancer Res* 64:4064–4068.
26. Gonzalez E, Kou R, Michel T (2006) Rac1 modulates sphingosine 1-phosphate-mediated activation of phosphoinositide 3-kinase/Akt signaling pathways in vascular endothelial cells. *J Biol Chem* 281:3210–3216.
27. Irani K, Xia Y, Zweier JL, et al. (1997) Mitogenic signaling mediated by oxidants in Ras-transformed fibroblasts. *Science* 275:1649–1652.
28. Samper E, Nicholls DG, Melov S (2003) Mitochondrial oxidative stress causes chromosomal instability of mouse embryonic fibroblasts. *Aging Cell* 2:277–285.
29. Suh YA, Arnold RS, Lassegue B, et al. (1999) Cell transformation by the superoxide-generating oxidase Mox1. *Nature* 401:79–82.
30. Droge W (2002) Free radicals in the physiological control of cell function. *Physiol Rev* 82:47–95.
31. Hirota K, Semenza GL (2001) Rac1 activity is required for the activation of hypoxia-inducible factor 1. *J Biol Chem* 276:21166–21172.
32. Borras C, Sastre J, Garcia-Sala D, et al. (2003) Mitochondria from females exhibit higher antioxidant gene expression and lower oxidative damage than males. *Free Radical Biol Med* 34:546–552.
33. Weich HA, Salahuddin SZ, Gill P, et al. (1991) AIDS-associated Kaposi's sarcoma-derived cells in long-term culture express and synthesize smooth muscle alpha-actin. *Am J Pathol* 139:1251–1258.
34. Darby I, Skalli O, Gabbiani G (1990) Alpha-smooth muscle actin is transiently expressed by myofibroblasts during experimental wound healing. *Lab Invest* 63:21–29.
35. Simonart T, Hermans P, Schandene L, Van Vooren JP (2000) Phenotypic characteristics of Kaposi's sarcoma tumour cells derived from patch-, plaque- and nodular-stage lesions: Analysis of cell cultures isolated from AIDS and non-AIDS patients and review of the literature. *Br J Dermatol* 143:557–563.
36. Gao P, Zhang H, Dinavahi R, et al. (2007) HIF-dependent antitumorigenic effect of antioxidants in vivo. *Cancer Cells* 12:230–238.
37. Albini A, Morini M, D'Agostini F, et al. (2001) Inhibition of angiogenesis-driven Kaposi's sarcoma tumor growth in nude mice by oral N-acetylcysteine. *Cancer Res* 61:8171–8178.
38. Mucomyst [package insert] (2001) (Bristol Meyers Squibb, Princeton, NJ).
39. Munzel T, Afanas'ev IB, Kleschyov AL, Harrison DG (2002) Detection of superoxide in vascular tissue. *Arterioscler Thromb Vasc Biol* 22:1761–1768.
40. Reiner A, Yekutieli D, Benjamini Y (2003) Identifying differentially expressed genes using false discovery rate controlling procedures. *Bioinformatics* 19:368–375.